Condensation of Fermions in the double-well potential*

Chen Xin-Wei(陈欣委), Liu Zhong-Qiang(刘中强), and Kong Xiang-Mu(孔祥木)†

College of Physics and Engineering, Qufu Normal University, Qufu 273165, *China*

(Received 22 April 2013; revised manuscript received 11 June 2013; published online 10 December 2013)

The density distribution of ultracold two-component fermionic gases ^{6}Li, which are confined in a gradient magnetic field and a symmetrical double-well potential, is investigated by employing local-density approximation. It is found that three different regimes including quasi-molecular Bose–Einstein condensation (BEC_m), the dimers in the unitarity limit (UL_d), and Bardeen–Cooper–Schrieffer superfluid (BCS) can coexist at the same time. Furthermore, the ranges of these regimes can be controlled to some extent by tuning the gradient of the magnetic field and the parameters characterizing the properties of the double-well potential. This study is of guidance and significance for experimentally realizing the coexistence of BEC_m, UL_d, and BCS in the double-well potential.

Keywords: molecular Bose–Einstein condensation, unitarity limit, Bardeen–Cooper–Schrieffer superfluid

PACS: 67.10.Db, 67.85.Lm, 03.75.Ss **DOI:** 10.1088/1674-1056/23/2/026701

1. Introduction

In 1925, Einstein predicted[1] that, below a certain temperature a finite fraction of the number of gas particles begins to condense into the ground state. Much attention and effort has since been focused on the research of Bose–Einstein Condensation (BEC), both experimentally and theoretically.[2–4] In 1995 the phenomenon of BEC was finally realized in the laboratory.[5–7] It is well known that fermions cannot form BEC directly. However, when there are interactions among fermions it is possible for fermions to form BEC. The strength of these interactions are usually characterized by the s-wave scattering length a, and they are repulsive when $a < 0$ and attractive when $a > 0$. Recent investigations show that Feshbach resonance[8] makes it possible to realize the crossover from the BEC of molecules to the superfluid, as described by the Bardeen–Cooper–Schrieffer (BCS) model.[9–11] The crossover has been investigated from different viewpoints; for example, the condensate fraction,[12,13] collective excitation,[14–16] and quantum pressure correction to the collective excitation spectrum.[17] Moreover, with the rapid development of the Feshbach resonance technology and the cryogenic cooling technology, some groups have observed the phenomena of BEC in fermionic atoms, such as ^{40}K[18] and ^{6}Li,[19,20] which provides a new way to study ultracold fermions.

Recently, for the ultracold two-component fermionic gases ^{6}Li, the coexistence of quasi-molecular BEC (BEC_m), the strongly interacting fermionic dimers in the unitarity limit (UL_d), and the BCS superfluid have been predicted.[20] Here, ^{6}Li atoms located in a harmonic potential are trapped in a uniform gradient magnetic field near the Feshbach resonance.[21] Since a large number of experiments have recently been performed upon atomic BEC trapped in the double-well potential,[22–27] and there are several tunable parameters to change the properties of the double-well potential, we can expect that the controllability of different regimes for fermionic gases ^{6}Li can be improved by introducing the double-well potential. To check our conjecture, in the present work we study the density distribution of the two-component fermionic gases ^{6}Li trapped in a symmetrical double-well potential. Meanwhile, an external magnetic field near the Feshbach resonance is applied to these gases. Our results predict the coexistence of the above three states, and the ranges of these states can be controlled to some extent by tuning the gradient of the magnetic field. Besides, tuning the parameters characterizing the properties of the double-well potential can control both the density distributions and the ranges of these states, to a certain degree.

The remainder of this paper is organized as follows. Section 2 describes the basic model and main calculations. We will focus on the density distributions in various regions. Section 3 shows the results of density distributions of the three different states and the corresponding discussion. Finally, a summary is given in Section 4.

2. Basic model and calculations

For fermionic atoms ^{6}Li, there are two different internal states, which can be characterized by expressions $|1\rangle = |f = 1/2, m_f = -1/2\rangle$ and $|2\rangle = |f = 1/2, m_f = 1/2\rangle$, where f is the total atomic spin and m_f is the spin projection quantum number. The interactions between $|1\rangle$ and $|2\rangle$ can be described by the s-wave scattering length a. In this work, we suppose that the two-component fermionic gases ^{6}Li are trapped

*Project supported by the National Natural Science Foundation of China (Grant No. 11275112), the Natural Science Foundation of Shandong Province of China (Grant No. ZR2011AM018), and the Specialized Research Fund for the Doctoral Program of Higher Education of China (Grant No. 20103705110004).

†Corresponding author. E-mail: kongxm@mail.qfnu.edu.cn

© 2014 Chinese Physical Society and IOP Publishing Ltd

in a gradient magnetic field $\boldsymbol{B} = (B_0 + \alpha z)\, \boldsymbol{e}_x$, where B_0 is the magnetic field at which the Feshbach resonance peaks, α is the magnetic field gradient, z is the coordinate, and $\boldsymbol{e}_x$ is a unit vector in the x direction. For ^{6}Li described above, the scattering length near B_0 is[21]

$$a(z) = Aa_0\left(1 - \frac{\omega}{B - B_0}\right). \tag{1}$$

Here A is a constant, a_0 is the Bohr radius, and ω is the width of the resonant magnetic field. According to Eq. (1), the scattering length $a(z)$ is very large in the vicinity of the Feshbach resonance; that is, $a(z) \to -\infty$ on one side of the resonance and $a(z) \to +\infty$ on the other side. This means that there are strongly repulsive interactions among atoms on one side of the resonance and strongly attractive interactions on the other side. According to Ref. [28], for different values of $a(z)$ the space can be divided into three regions, which correspond to three different states. They are $\mathrm{BEC_m}$, $\mathrm{UL_d}$, and BCS. Their boundaries are determined by $|a(z)|\, n^{1/3} = 1$ (n is the average particle density, and $n^{-1/3}$ represents the average distance between particles, while $|a(z)|$ denotes the range of the interaction).

Considering that the ultracold two-component fermionic gases ^{6}Li are confined in a symmetrical double-well potential, we can illustrate the general features of the double-well potential by the following form[29]

$$V_{\mathrm{opt}} = \gamma m\left(z^2 - \frac{\omega_z^2}{8\gamma}\right)^2 + \frac{1}{2}m\omega_{\mathrm{r}}^2\left(x^2 + y^2\right), \tag{2}$$

where γ is the tunable parameter, ω_z is the trap frequency in the z direction, and ω_{r} is the trap frequency in the x–y plane. Obviously, a double-well potential contains two potential wells which are separated by a barrier. According to Eq. (2), the height of the middle barrier is $m\omega_z^4/64\gamma$ at $z = 0$. The bottoms of the two wells are separately located at $z = -\sqrt{\omega_z^2/8\gamma}$ and $z = \sqrt{\omega_z^2/8\gamma}$, which means that the distance between the two wells is $2\sqrt{\omega_z^2/8\gamma}$. Figures 1(a) and 1(b) plot the results for the coordinate z dependence of the double-well potential for various values of the parameter γ and the trap frequency in the z direction ω_z, respectively (V_{opt} is in unit of 10^{-31} J, and γ is in unit of $\mathrm{m^{-2}{\cdot}s^{-2}}$). As shown in Fig. 1(a), as the parameter γ increases, the bottoms of the two wells approach each other, and the height of the barrier becomes shorter. Thus, the double wells become more unobvious. However, the influence of ω_z on the property of the double-well potential is contrary to the parameter γ, which can be seen from Fig. 1(b): as ω_z increases, the bottoms of the two wells go far away from each other, and the height of the barrier becomes higher, which indicates that the double wells become more obvious.

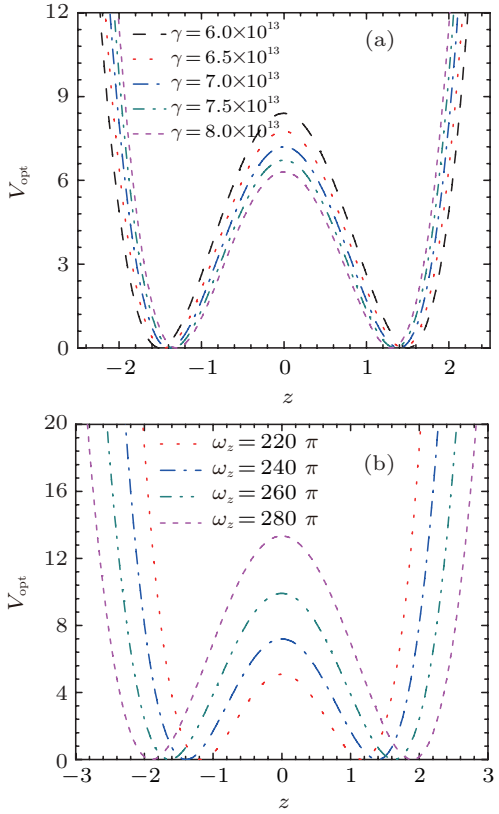


Fig. 1. (color online) The relationship between the double-well potential V_{opt} (V_{opt} is in unit of 10^{-31} J) and the coordinate z with different values of (a) the parameter γ for the case of $\omega_z = 240\,\pi$ and (b) the trap frequency in the z direction ω_z for the case of $\gamma = 7.0 \times 10^{13}$ $\mathrm{m^{-2}{\cdot}s^{-2}}$.

Since the crossover from BEC to BCS occurs near the Feshbach resonance, which appears at $z = 0$, the parameter γ should ensure that the distance is not too large and also make the two wells obvious enough in a certain range. Thus, we chose the parameter γ varying from 6.0×10^{13} $\mathrm{m^{-2}{\cdot}s^{-2}}$ to 8.0×10^{13} $\mathrm{m^{-2}{\cdot}s^{-2}}$. When ω_{r} is large enough, in the x–y plane most of the particles are gathered near the origin $(0,0)$. Since there is no magnetic field gradient in the directions of both x and y, setting $x = y = 0$ is a reliable method to ignore the affection coming from the x–y plane. In this case, the external potential for the fermionic atom ^{6}Li in the internal state $|i\rangle$ ($i = 1, 2$) is

$$V_{|i\rangle} = V_{\mathrm{opt}} - \boldsymbol{\mu}_{|i\rangle} \cdot \boldsymbol{B} = \gamma m z^4 - \frac{m\omega_z^2}{4}z^2 + \frac{m\omega_z^4}{64\gamma} - \boldsymbol{\mu}_{|i\rangle} \cdot \boldsymbol{B}, \tag{3}$$

and for molecule $^6\mathrm{Li}_2$, the total external potential is[21]

$$V_{\mathrm{m}} = 2\gamma m z^4 - \frac{m\omega_z^2}{2}z^2 + \frac{m\omega_z^4}{32\gamma} - \boldsymbol{\mu}_{\mathrm{m}} \cdot \boldsymbol{B}. \tag{4}$$

The last term in Eq. (3), which has the same physical meaning as the last term in Eq. (4), denotes the Zeeman energy. However, $\boldsymbol{\mu}_{|i\rangle}$ in Eq. (3) is the magnetic moment of the internal state $|i\rangle$ and $\boldsymbol{\mu}_{\mathrm{m}}$ in Eq. (4) is the magnetic moment of the molecule.

When the gases, which are trapped in the double-well potential and confined in the external magnetic field, reach their thermal and chemical equilibrium, the size of the paired atoms

is much smaller than the size of the Fermi cloud. Thus, the local-density approximation can be used to calculate the density distribution of each region.

The chemical potentials of $\mathrm{BEC_m}$, $\mathrm{UL_d}$, and $\mathrm{BCS}_{|i\rangle}$ are obtained as follows:[30,31]

$$\mu_{\mathrm{m}}^{\mathrm{BEC}} = g_{\mathrm{mm}} n_{\mathrm{m}}^{\mathrm{BEC}} + V_{\mathrm{m}}^{'} + \varepsilon_{\mathrm{m}}, \tag{5}$$

$$\mu_{\mathrm{d}}^{\mathrm{UL}} = \varepsilon_{\mathrm{Fm}}(\boldsymbol{r}) + V_{\mathrm{mf}}(\boldsymbol{r}) + \sum_i V_{|i\rangle}(\boldsymbol{r}), \tag{6}$$

and

$$\mu_{|i\rangle}^{\mathrm{BCS}} = \frac{\hbar^2 (6\pi^2)^{2/3}}{2m} \left(n_{|i\rangle}^{\mathrm{BCS}}\right)^{2/3} + V_{|i\rangle}. \tag{7}$$

Here, $g_{\mathrm{mm}} = 2\pi\hbar^2 a_{\mathrm{m}}(z)/m_{\mathrm{m}}$ is the molecule–molecule coupling with $a_{\mathrm{m}}(z) = 0.6a(z)$[32] being molecule–molecule scattering length and m_{m} being the reduced mass of the molecule, $V_{\mathrm{m}}^{'} = \sum_i V_{|i\rangle}$ denotes the total external potential of the two different atoms that combine into a molecule, $\varepsilon_{\mathrm{m}} = -\hbar^2/ma^2(z)$ is the binding energy of the molecule; $\varepsilon_{\mathrm{Fm}}(\boldsymbol{r}) = \hbar^2 (6\pi^2)^{2/3} \left(n_{\mathrm{d}}^{\mathrm{UL}}\right)^{2/3}/2m_{\mathrm{m}}$ represents the local Fermi energy, $V_{\mathrm{mf}}(\boldsymbol{r}) = \beta\varepsilon_{\mathrm{Fm}}(\boldsymbol{r})$ is the mean-field contribution to the chemical potential, and $n_{\mathrm{m}}^{\mathrm{BEC}}$, $n_{\mathrm{d}}^{\mathrm{UL}}$, and $n_{|i\rangle}^{\mathrm{BCS}}$ are the density distributions of the molecular BEC, the unitarity limit regime, and the fermionic atoms ^{6}Li in the BCS regime, respectively.

Equations (5)–(7) present the chemical potentials of different particles. As the magnetic field B increases, the distance between the two tight-binding atoms becomes larger and larger, making the quasi-molecules begin to evolve into dimer, and then the dimers begin to evolve into two atoms.[33] When the whole system achieves thermal and chemical equilibrium, the chemical potentials of molecules, dimers, and the two atoms have the same value μ_{sys} (the chemical potential of the whole system); that is,

$$\mu_{\mathrm{m}}^{\mathrm{BEC}} = \mu_{\mathrm{d}}^{\mathrm{UL}} = \sum_i \mu_{|i\rangle}^{\mathrm{BCS}} = \mu_{\mathrm{sys}}. \tag{8}$$

From Eqs. (5)–(7) one can get the density distribution of each regime based on the determination of $\mu_{\mathrm{sys}} \equiv \mu_{\mathrm{d}}^{\mathrm{UL}}(\boldsymbol{r}=0)$ and $\mu_{\mathrm{sys}} = \mu_{\mathrm{eff}} + \sum_i V_{|i\rangle}(\boldsymbol{r}=0)$. The density distributions of the three regions are given as follows:

$$n_{\mathrm{m}}^{\mathrm{BEC}} = \frac{m\left(\mu_{\mathrm{eff}} + \dfrac{\hbar^2}{ma^2(z)} - 2\gamma m z^4 + \dfrac{m\omega_z^2}{2} z^2\right)}{1.2\pi\hbar^2 a(z)}, \tag{9}$$

$$n_{\mathrm{d}}^{\mathrm{UL}} = \left[\frac{4m\left(\mu_{\mathrm{eff}} - 2\gamma m z^4 + \dfrac{m\omega_z^2}{2} z^2\right)}{(1+\beta)\hbar^2 (6\pi^2)^{2/3}}\right]^{3/2}, \tag{10}$$

and

$$n_{|i\rangle}^{\mathrm{BCS}} = \left[\frac{m\left(\mu_{\mathrm{eff}} - 2\gamma m z^4 + \dfrac{m\omega_z^2}{2} z^2\right)}{\hbar^2 (6\pi^2)^{2/3}}\right]^{3/2}. \tag{11}$$

3. Results and discussion

In this section, we present the results of density distributions obtained from Eqs. (9)–(11), and discuss the effects of the gradient α, the parameter γ, and the trap frequency in the z direction ω_z. The order of magnitude of the parameter γ is determined by the double-well potential V_{opt}, the coordinate z, the angular frequency ω_z, and the mass of the particle trapped in the double-well potential m. Our calculation indicates that, when the order of magnitude of the parameter γ is thirteen, we can get some interesting results. When the order of magnitude of the parameter γ is much smaller, the term containing the parameter γ can be neglected, which can be seen from Eqs. (9)–(11); when the order of magnitude of the parameter γ is much larger, the density distribution will be negative. To get the curves of the density distributions, we set $n_{\mathrm{d}}^{\mathrm{UL}}(\boldsymbol{r}=0) = 10^{12}$ cm^{-3}. The values of $A\omega$ (in Eq. (1)) and β are estimated as follows: $A\omega = 6$ Gs (1 Gs = 10^{-4} T)[34] and $\beta = -0.3$.[13,35] Under the parameter of $m = 9.98 \times 10^{-27}$ kg, one can get the following results (the density distribution is in unit of $n_{\mathrm{d}}^{\mathrm{UL}}(\boldsymbol{r}=0)$ and the coordinate z is in unit of $R_z = \sqrt{\mu_{\mathrm{sys}}/m(240\pi)^2}$ for simplicity).

According to Fig. 1 choosing $\gamma = 7.0 \times 10^{13}$ m^{-2}·s^{-2}, $\omega_z = 240\ \pi$ and employing Eq. (9), we plot Fig. 2, which shows the curves of the coordinate z dependence of the molecular density distribution with different values of the gradient α in the BEC regime. As shown in Fig. 2, when z increases to zero, the density $n_{\mathrm{m}}^{\mathrm{BEC}}$ increases from zero to a maximum $n_{\mathrm{max}}^{\mathrm{BEC}}$ and then decreases to zero. Moreover, the growth rate is much larger than the reduction rate. The peak located in the left region of the whole BEC region indicates that most of the BEC molecules distribute in the left part of the left well. It is obvious that the magnetic field gradient α has an observable effect on the range of the BEC region: when α increases, the range of the BEC region becomes larger and larger. Figure 2 exhibits that $n_{\mathrm{max}}^{\mathrm{BEC}}$ increases with the increasing α. From the

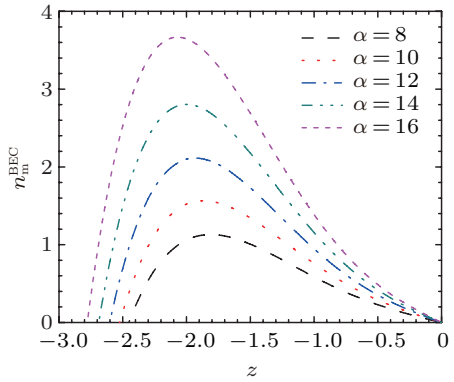


Fig. 2. (color online) The density distribution of quasi-molecular BEC as a function of the coordinate z for $\alpha = 8$, 10, 12, 14, and 16 Gs·m^{-1} (1 Gs = 10^{-4} T) with the given values of $\gamma = 7.0 \times 10^{13}$ m^{-2}·s^{-2} and $\omega_z = 240\ \pi$.

above results and discussion, we know that it is much easier to form molecular BEC when the gradient α is larger. When $|\boldsymbol{B}| < B_0$, we can control the axial width of the BEC region to some degree by adjusting the magnetic gradient α. This may be a reliable method that can contribute to realizing the condensation of fermions ^{6}Li.

Using Eqs. (9)–(11), one can obtain Figs. 3(a), 3(b), and 3(c) by setting $\alpha = 12$ Gs/m and $\omega_z = 240\ \pi$, and obtain Figs. 3(d), 3(e), and 3(f) by setting $\alpha = 12$ Gs/m and $\gamma = 7.0 \times 10^{13}$ m^{-2}·s^{-2}. Figure 3(a) exhibits that $n_{\max}^{\mathrm{BEC}}$ decreases with the increasing γ. While figure 3(d) exhibits that the trap frequency ω_z has no influence on $n_{\max}^{\mathrm{BEC}}$. The density distribution of the condensed molecules has a single-peak structure (see Figs. 3(a) and 3(d)), while the density distributions in the $\mathrm{UL_d}$ and $\mathrm{BCS}_{|i\rangle}$ regions have a double-peak structure (see Figs. 3(b), 3(c), 3(e), and 3(f)). Moreover, two peaks correspond to the bottoms of the two wells of the potential. For given values of gradient α, tuning the parameters γ and ω_z can change the properties of the double-well potential, as shown in Fig. 1. This results in the changes of the axial width of the three regions and the density distributions in them. Figure 3 exhibits the related results. The axial widths of $\mathrm{BEC_m}$, $\mathrm{UL_d}$, and $\mathrm{BCS}_{|i\rangle}$ become smaller and smaller as γ increases. While for given values of gradient α and γ, as ω_z decreases, the changing trends of the curves are similar to those in the case with increasing γ. This can be seen from Figs. 3(d), 3(e), and 3(f). However, when z approaches zero, the effects of the parameter γ and the trap frequency ω_z become unobvious: different curves overlap near the origin. At $z = 0$, the magnetic field satisfies $\boldsymbol{B} = B_0 e_x$, where the Feshbach resonance

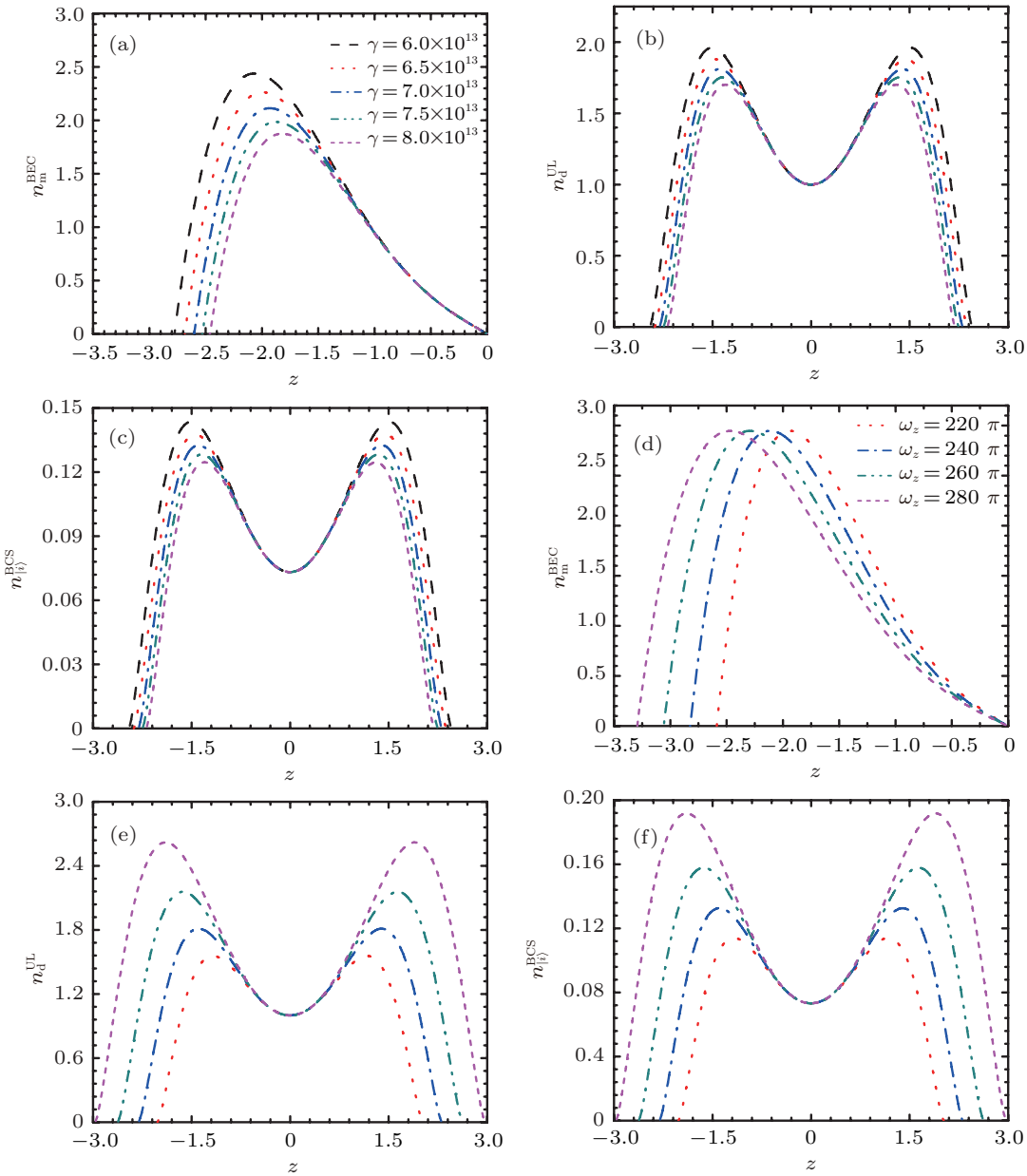


Fig. 3. (color online) Comparisons of the density distributions in different regions as a function of the coordinate z for different γ and ω_z with the given value of $\alpha = 12$ Gs/m: panels (a) and (d) show the density distributions of the quasi-molecular BEC; panels (b) and (e) give the density distributions in the unitarity limit regime; panels (c) and (f) exhibit the density distributions of the fermionic atoms ^{6}Li in the BCS regime.

occurs. Compared with the region away from the Feshbach resonance, the effects of γ and ω_z are weakened near the Feshbach resonance. From the above discussion, we can conclude that, besides the gradient of the magnetic field α, the parameter γ and the trap frequency ω_z can also be used to tune the axial widths of $\mathrm{BEC_m}$, $\mathrm{UL_d}$, and $\mathrm{BCS}_{|i\rangle}$.

Setting $\alpha = 12$ Gs/m, $\gamma = 7.0 \times 10^{13}$ m^{-2}·s^{-2}, and $\omega_z = 240\,\pi$, the density distribution of the particles in each regime is plotted in Fig. 4. This shows that fermionic gases in forms of $\mathrm{BEC_m}$, $\mathrm{UL_d}$, and $\mathrm{BCS}_{|i\rangle}$ can coexist at the same time in different regions. According to $|a(z)|n^{1/3} = 1$, the vertical lines located at $z = -1.223\ R_z$ and $z = 1.0983\ R_z$ in Fig. 4 denote the boundaries of the three regimes: I, II, and III represent the regions of $\mathrm{BEC_m}$, $\mathrm{UL_d}$, and $\mathrm{BCS}_{|i\rangle}$, respectively. The middle barrier of the double-well potential isolates the molecular BEC from the atomic BCS. Actually, as the magnitude of the magnetic field B increases, the distance between the two tight-binding atoms becomes larger and larger, making the molecules evolve into dimmers and Cooper pairs, subsequently. Furthermore, the Cooper pairs could form a BCS superfluid when B is large enough. In other words, if the applied magnetic field has a uniform gradient, the three states of fermionic gases can coexist at the same time.

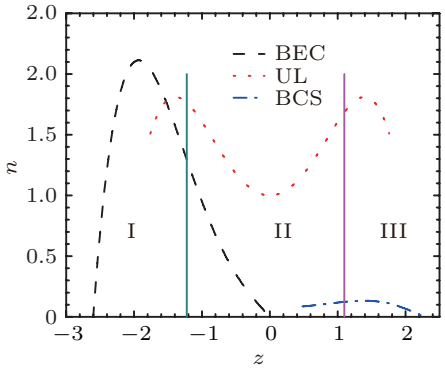


Fig. 4. (color online) The density distribution of each regime for the case of $\alpha = 12$ Gs/m, $\gamma = 7.0 \times 10^{13}$ m^{-2}·s^{-2}, $\omega_z = 240\,\pi$, and the boundaries of the regions of $\mathrm{BEC_m}$, $\mathrm{UL_d}$, and $\mathrm{BCS}_{|i\rangle}$ (vertical lines).

4. Summary

This work has employed the local-density approximation to study the density distribution of two-component ultracold Fermi gases ^{6}Li trapped in a gradient magnetic field and a symmetrical double-well potential. Three important states, including $\mathrm{BEC_m}$, $\mathrm{UL_d}$, and $\mathrm{BCS}_{|i\rangle}$, are obtained by the scattering theory and the Feshbach resonance theory. We have analyzed in detail the density distributions in the three regimes, especially in the molecular BEC regime. It is found that the gradient of the magnetic field α, the parameter γ, and the trap frequency in the z direction ω_z have an influence on the density distribution of the condensed molecules $^6\mathrm{Li}_2$. Moreover, γ and ω_z may affect the density distributions of $\mathrm{UL_d}$, and $\mathrm{BCS}_{|i\rangle}$. Consequently, by tuning the gradient of the magnetic field α, the parameter γ, and the trap frequency in the z direction ω_z, one can to some degree control the ranges of the three regimes. This provides a pathway for experimentally realizing the coexistence of $\mathrm{BEC_m}$, $\mathrm{UL_d}$, and $\mathrm{BCS}_{|i\rangle}$ in the double-well potential.

References

[1] Einstein A 1925 *Sitz. Ber. Preuss. Akad. Wiss.* **1** 3
[2] London F 1938 *Phys. Rev.* **54** 947
[3] Hecht C E 1959 *Physica* **25** 1159
[4] Silvera I F and Walraven J T M 1980 *Phys. Rev. Lett.* **44** 164
[5] Anderson M H, Ensher J R, Matthews M R, Wieman C E and Cornell E A 1995 *Science* **269** 198
[6] Davis K B, Mewes M O, Andrews M R, Druten N J V, Durfee D S, Kurn D M and Ketterle W 1995 *Phys. Rev. Lett.* **75** 3969
[7] Bradley C C, Sackett C A, Tollett J J and Hulet R G 1995 *Phys. Rev. Lett.* **75** 1687
[8] Donley E A, Claussen N R, Thompson S T and Wieman C E 2002 *Nature* **417** 529
[9] Timmermans E, Furuya K, Milonni P W and Kerman A K 2001 *Phys. Lett. A* **285** 228
[10] Holland M, Kokkelmans S J J M F, Chiofalo M L and Walser R 2001 *Phys. Rev. Lett.* **87** 120406
[11] Milstein J N, Kokkelmans S J J M F and Holland M J 2002 *Phys. Rev. A* **66** 043604
[12] Regal C A, Greiner M and Jin D S 2004 *Phys. Rev. Lett.* **92** 040403
[13] Zwierlein M W, Stan C A, Schunck C H, Raupach S M F, Kerman A J and Ketterle W 2004 *Phys. Rev. Lett.* **92** 120403
[14] Kinast J, Hemmer S L, Gehm M E, Turlapov A and Thomas J E 2004 *Phys. Rev. Lett.* **92** 150402
[15] Bartenstein M, Altmeyer A, Riedl S, Jochim S, Chin C, Denschlag J H and Grimm R 2004 *Phys. Rev. Lett.* **92** 203201
[16] Ma X D, Yang Z J, Lu J Z and Wei W 2011 *Chin. Phys. B* **20** 070307
[17] Dong H and Ma Y L 2009 *Chin. Phys. B* **18** 715
[18] Greiner M, Regal C A and Jin D S 2003 *Nature* **426** 537
[19] Jochim S, Bartenstein M, Altmeyer A, Hendl G, Riedl S, Chin C, Denschlag J H and Grimm R 2003 *Science* **302** 2101
[20] Zwierlein M W, Stan C A, Schunck C H, Raupach S M F, Gupta S, Hadzibabic Z and Ketterle W 2003 *Phys. Rev. Lett.* **91** 250401
[21] Xiong H W, Liu S J, Zhang W P and Zhan M S 2005 *Phys. Rev. Lett.* **95** 120401
[22] Shin Y, Saba M, Pasquini T A, Ketterle W, Pritchard D E and Leanhardt A E 2004 *Phys. Rev. Lett.* **92** 050405
[23] Schumm T, Hofferberth S, Andersson L M, Wildermuth S, Groth S, Bar-Joseph I, Schmiedmayer J and Kruger P 2005 *Nat. Phys.* **1** 57
[24] Mahmud K W, Perry H and Reinhardt W P 2005 *Phys. Rev. A* **71** 023615
[25] Shomroni I, Lahoud E, Levy S and Steinhauer J 2009 *Nat. Phys.* **5** 193
[26] LeBlanc L J, Bardon A B, McKeever J, Extavour M H T, Jervis D and Thywissen J H 2011 *Phys. Rev. Lett.* **106** 025302
[27] Wang W Y, Yang Y, Meng H J, Ma Y, Qi P T, Ma Y Y and Duan W S 2012 *Acta Phys. Sin.* **61** 100301 (in Chinese)
[28] Bourdel T, Khaykovich L, Cubizolles J, Zhang J, Chevy F, Teichmann M, Tarruell L, Kokkelmans S J J M F and Salomon C 2004 *Phys. Rev. Lett.* **93** 050401
[29] Milburn G J, Corney J, Wright E M and Walls D F 1997 *Phys. Rev. A* **55** 4318
[30] Gehm M E, Hemmer S L, Granade S R, O′Hara K M and Thomas J E 2003 *Phys. Rev. A* **68** 011401
[31] Carr L D, Chiaramonte R and Holland M J 2004 *Phys. Rev. A* **70** 043609
[32] Petrov D S, Salomon C and Shlyapnikov G V 2004 *Phys. Rev. Lett.* **93** 090404
[33] Ho T L 2004 *Science* **305** 1114
[34] Strecker K E, Partridge G B and Hulet R G 2003 *Phys. Rev. Lett.* **91** 080406
[35] O′Hara K M , Hemmer S L, Gehm M E, Granade S R and Thomas J E 2002 *Science* **298** 2179